

# Mechanical Properties Optimization and Modeling of Palm Kernel Shell Ash Reinforced Al-Mg-Si Composite using Grey Relational Analysis

Elijah Oyewusi Oyedeji<sup>1,2,\*</sup> | Muhammed Dauda<sup>1,3</sup> |  
Shehu Aliyu Yaro<sup>4</sup> | Malik Abdulwahab<sup>4,5</sup>

<sup>1</sup>Department of Mechanical Engineering, Ahmadu Bello University, Zaria, Nigeria

<sup>2</sup>National Space Research and Development Agency (NASRDA), Abuja, Nigeria

<sup>3</sup>Provost office, Airforce Institute of Technology, Kaduna, Nigeria

<sup>4</sup>Department of Metallurgical and Materials Engineering, Ahmadu Bello University, Zaria, Nigeria

<sup>5</sup>Department of Metallurgical and Materials Engineering, Faculty of Air Engineering, Airforce Institute of Technology, Kaduna, Nigeria

\*Corresponding author: [foladeji1@gmail.com](mailto:foladeji1@gmail.com)

Received 28 March 2022; Revised 22/27 April 2022; Accepted 29 May 2022

**Abstract:** There is relatively little information on the mechanical behavior and modeling of palm kernel shell ash reinforced Al-Mg-Si composite. Thus, this study investigates the mechanical behavior and modeling of Al-Mg-Si composite. Hardness, impact strength and modulus of rupture (MOR) of the composite were investigated and analyzed using Minitab 16 and Origin software. It was found that the mechanical properties of the composite are inconsistent with composition variation. The mathematical and graphical modeling of the composite mechanical properties of the composite have been presented. The modeling revealed that aside the composition, there are other factors responsible for the mechanical behavior of the composite which were not considered in the experimental analysis. Validation of the claim was also made with analysis. The study of the interaction between the two compositions on the resultant mechanical properties gave some specific compositions with better mechanical properties. However, this study strongly recommends conduction of further analysis on other important factors responsible for the mechanical response of the composite.

**Keywords:** Multi-objective optimization; mechanical properties; preferable probability; grey relational analysis; Al-Mg-Si composite

## 1. Introduction

Achieving both strength and flexibility in designing materials simultaneously is turning out to be progressively challenging. On account of lightweight Al composites, grain refinement utilizing grain refinement strategies such as high-pressure torsion, friction stir processing (FSP), and equal, which are key examples of plastic deformation strategies, have proved to produce ultrafine-grained (UFG) Al-composite with higher strength (Edalati *et al.*, 2012; Li *et al.*, 2018; Sanchez *et al.*, 2021). However,

ductility is reduced in the case of coarse-grained Al-composite due to the presence of low dislocation and disjointed coalesce, creating accumulating capabilities due to grain particle size and dispersion within the composition (Oyedemi et al., 2021a; 2021b; 2021c). The presence of second-phase particles can significantly increase dislocation accumulation ability and resistance to dislocation sliding; therefore, adding some particles to the UFG matrix is one alternative. AA7075 has been cryogenically rolled (Kazemi-Navaee et al., 2021), age-hardenable AA6063 (Engler, 2022), AA6082 alloys (Rakhmonov et al., 2021), and in other cases, nano-particles have been used to reinforced Al composites (Chakravarthy et al., 2020). All of these methods are some of the ways that the addition of second-phase particles has helped improve the strength and flexibility of Al-composite based on literature.

Aluminium is the third most plentiful element on the planet (Chaudhary & Tak, 2022). It has fundamentally supplanted ferrous components in the scope of uses because of its remarkable properties, which include low density that is responsible for its lightweight and resistance to corrosion as a result of its passivation characteristics. However, there are some disadvantages when Aluminum is used alone for some industrial applications (Kulekci, 2008; Sharma et al., 2021). To fix and combat defects/imperfections/irregularities in pure aluminium, the combinations of the pure Al with other materials leading to the formation of another material known as Al-composite was found. An example of the Al-composite is the Al-Metallic Matrix Composite (MMC). An MMC is an intensified material made by joining two distinct parts to make a reinforced material. The constant material where the reinforcing material is consolidated, be it in the form of particles, textiles, or whiskers, is alluded to as the matrix of the MMC (Chou et al., 1985). Furthermore, the reinforcing material can also be in the form of continuous or discontinuous particles. The term "hybrid metal matrix composite" (HMMC) refers to a material that contains more than one reinforcing element in addition to the matrix. MMCs assume a significant part in our day to day routines as materials that are mostly in use are made from MMCs. Some of the examples of reinforcing materials used in MMCs to develop mechanical structures are tungsten carbides, metallic binders, graphites, among others. When a typical material fails to fulfill the proper standards or specifications, it is usually used. The needed attribute to be reached with a base metal determines the metal matrix's reinforcement. MMCs in the form of Particulate Metal Matrix Composites (PMMCs) are a type of MMC (Kordijazi et al., 2021; Miracle, 2005).

Scholars have used the Grey Relational Analysis (GRA) model to achieve optimum parameters in the production of optimized materials with superior mechanical properties for engineering applications such as aircraft, automobiles, and chemical plants, among others. For instance, Pandya and Rathod (2020) used the GRA and were able to find the ideal composition of agricultural reinforcement materials to build polymer-matrix composites with good mechanical properties. Sumesh and Kanthavel (2020) produced optimum parameters for agricultural reinforcing materials, using the GRA approach and an artificial neural network. GRA has also been employed to optimize mechanical properties (Reddy & Chalamalasetti, 2021; Soorya Prakash et al., 2020). Thus, studies confirm the suitability of the GRA model for optimization problems (Yin, 2013).

The current study aims to learn about the mechanical behavior of Al-Mg-Si metal matrix reinforced by palm kernel shell ash (PKSA) produced through powder metallurgy using the GRA and statistical analysis. GRA was used to determine the ideal percentage weight composition of PKSA that gives the best mechanical qualities to obtain the best quality features. Section 1 contains the study's introduction and general background knowledge, section 2 contains materials and methods as they relate to this study, section 3 considers the study's experimental design, section 4 contains the experimental study's results and their discussions, and section 5 concluded the study.

## 2. Materials and methods

### 2.1 Materials and production

A palm oil processing plant in Nigeria, which is one of the major producers of oil palm, provided fresh palm kernel shells (Oyedemi et al., 2021a; Oyedemi et al., 2020). The fundamental Aluminum

6066 composite source was obtained from Shanghai Worldyang Chemical Co., Ltd., China, and comprised of unadulterated aluminum, manganese, silicon, chromium, magnesium, and copper powder. To act as reinforcement for the created aluminum matrix, the palm kernel shells were burned into ash. Details of the fabrication that took place between January 2020 and January 2021 exist in previous studies (Oyedemi et al., 2022).

To optimize mechanical properties based on the influence of PKSA reinforcement, the grey relational approach was utilized, which assessed performance attributes and normalized them from zero to one. This technique is known as grey relational generation. Using the normalized data, the grey relational coefficient was calculated. The Grey relational grade was then calculated by averaging the grey relational coefficients. The grey relationship grade determines the full response. A multi-response optimization problem is reduced to a single-response optimization problem using this strategy. The grey relational grade is the objective function (Ramu et al., 2018).

## 2.2 Mechanical Testing

**2.2.1 Hardness:** According to the ASTM E18-79 standard, the hardness of the composite was determined using the Rockwell hardness method with a force of 10 kgf.

**2.2.2 Impact strength:** The samples for the impact test were developed based on standard ISO-8256. Izod impact is a single point test that estimates material's resistance to impact from a pendulum. In this study, the Ceast Lot – Resil Impactor with Ceast NotchVIS was used. This test was carried out under standard conditions of relative air humidity and temperature of 50% and 23 °C respectively.

**2.2.3 Modulus of rupture:** The flexural strength test was performed by utilizing a Motorized Automatic Recording Tensometer. According to the ASTM D7028-07-201 standard, the samples were prepared, while the autographic recording drum of the machine was wrapped with the test graph sheet to record the readings of the test.

## 3. Experimental design

A palm oil processing plant in Nigeria, which is one of the major producers of oil palm, provided fresh palm kernel shells. The experiments are based on regression analysis, probability, and analysis of variance (ANOVA), with 11 experimental observations listed in Table 1.

### 3.1 Statistical analysis

The experimental mechanical properties were analyzed using regression analysis, analysis of variance (ANOVA), and interaction analysis with the help of Minitab (Version 16.1, Minitab Inc.) and Origin (Version 2020, OriginLab) software after the mechanical properties of the developed composites were evaluated. The percentage fluctuation in mechanical characteristics and the

**Table 1.** The experimental data

Experiment no.	PKSA	Al-Mg-Si	MOR (MPa)	Impact Strength (J)	Hardness
1	0	100	50.4	0.123	63.3
2	2.034	97.874	59.51	0.126	73
3	4.451	96.023	64.91	0.138	93
4	6.0323	93.9677	69.25	0.433	91
5	8.3902	82.7341	68.28	0.077	88
6	9.989	90.8879	56.32	0.138	91
7	12.781	88.0023	58.3	0.066	90.6
8	13.985	86.8745	64.84	0.111	73
9	15.997	83.9978	63.71	0.3	89
10	18.453	82.2348	56.81	0.21	82
11	20.0842	79.8765	60.07	0.013	0

descriptive statistical analysis of PKSA reinforcement on Al-Mg-Si alloy were computed in the study of Oyededeji *et al.* (2021c).

### 3.2 Grey relational analysis

Grey relational analysis is a popular method for determining the degree of link between sequences based on the grey relational grade. In recent times, some researchers have utilized GRA optimization method to optimize input parameters resulting in outputs responses based on the Grey relational grade (GRG). GRA is usually used to incorporate all of the desired performance qualities that are being examined into a solitary number that can be utilized as the single quality optimized conditions (Abifarin *et al.*, 2021; Ramu *et al.*, 2018). Based on the form of values for each of the output responses, normalization of optimization responses can be classified into three types. They are the 'the smaller the better', the 'nominal the better', and the 'higher the better' values (Girish *et al.*, 2019).

For this study, the high values for MOR, Impact Strength and Hardness are desirable for overall mechanical properties of the composite. Hence, 'higher the better' normalization criteria of Grey relational analysis (GRA) was utilized in the experimental step to generate grey grades and establish the response between zero and one. The grey relational coefficient (GRC) was calculated using the set data to illustrate how near the expected response is to the actual response. A grey relational grade (GRG) represents the overall evaluation of all the individual performance parameters, which is produced by averaging GRCs of all the performance parameters for each sample treatment (Abifarin *et al.*, 2021; Ramu *et al.*, 2018). Optimizing a single grey relational grade, for example, entails balancing a complex set of various performance criteria, with the highest grey relational grade-level serving as the ideal level of this process parameter (Abifarin *et al.*, 2021).

Equation 1 is the linear data preprocessing approach used in this work for the mechanical properties of the investigated composite, and the larger the criteria, the better.

$$x_i(k) = \frac{y_i(k) - \min y_i(k)}{\max y_i(k) - \min y_i(k)} \quad (1)$$

where  $x_i(k)$  is the preprocessed data,  $\min y_i(k)$  is the lowest  $y_i(k)$  response estimation,  $k^{\text{th}}$ , and  $\max y_i(k)$  is the greatest  $y_i(k)$  response estimation,  $k^{\text{th}}$ . The preprocessed data (grey relational generation sequences) from the experimental runs of the investigated composites are shown in Table 2.

Deng's grey relational analysis model was built to show the degree of grey relationship between two sequences  $[x_o(k)$  and  $x_i(k)$ ,  $i = 1, 2, 3, 4$ ;  $k = 1, 2 \& 3$ ]. The grey relational coefficient (GRC) is given by

$$\xi_i(k) = \frac{\Delta_{\min} + \zeta \Delta_{\max}}{\Delta_{oi}(k) + \zeta \Delta_{\max}} \quad (2)$$

where the deviation sequence is,

**Table 2.** The preprocessed observation data

Experiment no.	MOR (MPa)	Impact Strength (J)	Hardness
1	0	0.261905	0.680645
2	0.483289	0.269048	0.784946
3	0.769761	0.297619	1
4	1	1	0.978495
5	0.948541	0.152381	0.946237
6	0.314058	0.297619	0.978495
7	0.419098	0.12619	0.974194
8	0.766048	0.233333	0.784946
9	0.706101	0.683333	0.956989
10	0.340053	0.469048	0.88172
11	0.512997	0	0

$$\Delta_{oi}(k) = \| x_o(k) - x_i(k) \| \tag{3}$$

$\Delta_{oi}(k)$  denotes the difference in absolute value between  $x_o(k)$  and  $x_i(k)$ ,  $x_o(k)$  and  $x_i(k)$  denote the reference and similarity arrangements, respectively, and  $\zeta$  is the differentiating coefficient (0~1), which is generally allocated an equal weight of 0.5 to each parameter (Abifarin et al., 2021). The base of every reaction variable, as well as the majority of variations, are referred to as  $\Delta_{min}$  and  $\Delta_{max}$ . Table 3 presents the deviation sequence of the data in the experimental runs of the analyzed composites. The grey relationship coefficient (GRC), grey relational grade (GRG), and ranking are shown in Table 4 in which GRA was used to establish the GRG, and the respective value for each experiment number, ranking was carried out for the GRGs.

### 3.3 Probability-based multi-objective analysis

For aerospace applications, as previously stated in the GRA analysis, a considerable value of the mechanical qualities of the metallic composite is necessary; thus, the beneficial utility index technique was applied. In the computation, the index characteristic indicator contributes a linearly positive contribution to the partial preference probability (Ramu et al., 2018). Using Equation 4 and Equation 5, important parameters that relates to the partial probability index (denoted as  $P_{ij}$ ) and the normalized factor of the  $j^{th}$  utility index (denoted as  $\blacksquare_j$ ) were obtained to compute the performance characteristic indicator of the models.

$$P_{ij} = \blacksquare_{ij} x_{ij}; \quad i = 1, 2, \dots, n; j = 1, 2, \dots, m \tag{4}$$

$$\blacksquare_j = 1/(n\bar{x}_j) \tag{5}$$

Note that  $n$  and  $m$  are the sample number and utility indices of each sample respectively as it relate to this study,  $x_{ij}$  is the  $j$ th sample's characteristic performance beneficial utility index measurement, and  $\bar{x}_j$  is the value of the sample characteristic performance indicator's arithmetic mean utility index.

**Table 3.** The deviation sequence observation data

Experiment no.	MOR (MPa)	Impact Strength (J)	Hardness
1	1	0.738095	0.319355
2	0.516711	0.730952	0.215054
3	0.230239	0.702381	0
4	0	0	0.021505
5	0.051459	0.847619	0.053763
6	0.685942	0.702381	0.021505
7	0.580902	0.87381	0.025806
8	0.233952	0.766667	0.215054
9	0.293899	0.316667	0.043011
10	0.659947	0.530952	0.11828
11	0.487003	1	1

**Table 4.** Grey relational coefficients, grades and ranks

Experiment no.	MOR (MPa)	Impact Strength (J)	Hardness	Samples	GRG	Rank
1	0.333333	0.403846	0.610236	C1	0.449139	10
2	0.491782	0.40619	0.699248	C2	0.532407	9
3	0.684708	0.415842	1	C3	0.700183	4
4	1	1	0.958763	C4	0.986254	1
5	0.906686	0.371025	0.902913	C5	0.726874	2
6	0.421606	0.415842	0.958763	C6	0.598737	5
7	0.462577	0.363951	0.95092	C7	0.592483	6
8	0.681243	0.394737	0.699248	C8	0.591743	7
9	0.629803	0.612245	0.920792	C9	0.720947	3
10	0.431054	0.484988	0.808696	C10	0.574913	8
11	0.506584	0.333333	0.333333	C11	0.391084	11

Finally, the analysis' decisive preferred probability is calculated as the product of each candidate sample's partial preferable probability. During the ranking process, the candidate sample with the best performance characteristics is also determined. The composites' preferred probability optimization and ranking are shown in Table 5.

## 4. Results and discussion

### 4.1 Micro hardness analysis

The experimental hardness of the various samples with different compositions are displayed in Table 6. The results revealed an inconsistent pattern as the compositions change. The mathematical modeling of the experimental hardness is shown in Equation 6 using regression analysis. The experimental hardness and the modeled hardness are also displayed in Figure 1. The figure revealed that the modeled hardness is inconsistent with its corresponding experimental result.

$$\text{Hardness} = 135 - 1.85 \text{ PKSA} - 0.46 \text{ Al} - \text{Mg} - \text{Si} \quad (6)$$

The modeled hardness revealed the fitness of the experimental design. This shows that there are some factors that influenced the experimental hardness results obtained. The inconsistency is further supported by the analysis of variance (ANOVA) of the data as shown in Table 7. The table showed that the residual error was 63.5% as compared to the modeled data. The implication is that lots of errors or some factors have not been accounted for and this could be responsible to the hardness data of the composite. This means that a substantive conclusion cannot be drawn on the behavioral pattern of the hardness of the composite as the compositions vary. Hence, it is recommended in this study that other factors that may be responsible for hardness of the fabricated composite should be investigated.

It is important to understand the behavior of the resultant hardness value, relative to the interaction between Al-Mg-Si and PKSA. The results showed that barely from 82-96% Al-Mg-Si mixed with 6-11% of PKSA will give relatively higher hardness value compared to other

**Table 5.** Preferable probability optimization

Experiment no.	MOR (MPa)	Impact Strength (J)	Hardness	Pt*1000	Rank
1	0.074955	0.070893	0.075908	0.403365	9
2	0.088504	0.072622	0.08754	0.562655	6
3	0.096535	0.079539	0.111524	0.856313	4
4	0.102989	0.249568	0.109126	2.804839	1
5	0.101547	0.04438	0.105528	0.475582	8
6	0.08376	0.079539	0.109126	0.727013	5
7	0.086704	0.03804	0.108646	0.358344	10
8	0.096431	0.063977	0.08754	0.540067	7
9	0.09475	0.172911	0.106727	1.748549	2
10	0.084488	0.121037	0.098333	1.00558	3
11	0.089337	0.007493	0	0	11

**Table 6.** Experimental hardness data

Experiment no.	PKSA	Al-Mg-Si	Hardness
1	0	100	63.3
2	2.034	97.874	73
3	4.451	96.023	93
4	6.0323	93.9677	91
5	8.3902	82.7341	88
6	9.989	90.8879	91
7	12.781	88.0023	90.6
8	13.985	86.8745	73
9	15.997	83.9978	89
10	18.453	82.2348	82
11	20.0842	79.8765	0

compositions. Also, it is seen that 82-84% Al-Mg-Si mixed with 12-18% give a relatively higher hardness value. In addition, to the findings made above, in some instances a particular hardness value is desired for a particular application. Thus, these interactions are shown in Figure 2 with the specific compositions required for some specific hardness value.

#### 4.2 Impact strength analysis

Similar to hardness analysis, the experimental impact strength of the Al-Mg-Si-PKSA composites are presented in Table 8. It is noted that there is a gradient in impact strength of the composite as the composition varies. The mathematical modeling of the experimental impact strength is shown in Equation 7 obtained with the help of regression analysis. The experimental and the modeled impact strength are as shown in Figure 3. It is shown that the model impact strength does not follow the pattern of that of the experimental.

$$\text{Impact Strength (J)} = -0.67 + 0.0062 \text{ PKSA} + 0.0086 \text{ Al} - \text{Mg} - \text{Si} \quad (7)$$

The modeling revealed the unreliability of the repeatability of the experiment. The results showed that there are some factors responsible for the curation of the experimental impact strength of the composite that have been accounted for. ANOVA analysis (Table 9) further supports the inconsistency observed from the modeling. In the case of the contribution of the unaccounted factors on the experimental impact strength, the analysis revealed significant contribution of 81.7%. This is a pronounced contribution, which shows the necessity of further investigation of probable factors that may be responsible on the impact strength of the composite. These findings also showed that substantial conclusion cannot be drawn on the effect of the composition on the impact strength of the composite.

Figure 4 shows the interaction between Al-Mg-Si and PKSA relative to the resultant experimental impact strength. The results revealed that 92-95% Al-Mg-Si mixed with 4.5-6.5% of PKSA will give a relatively higher impact strength compared to other compositions. The presented interaction plot also highlights different compositions of Al-Mg-Si and PKSA with different resultant impact strength.

**Table 7.** Analysis of Variance for Hardness

Source	DF	SS	MS	% of Contribution
Modeled data	2	911.5	455.7	36.5
Residual Error	8	6344.6	793.1	63.5
Total	10	7256.0	1248.8	100

**Table 8.** Experimental impact strength

Experiment no.	PKSA	Al-Mg-Si	Impact Strength (J)
1	0	100	0.123
2	2.034	97.874	0.126
3	4.451	96.023	0.138
4	6.0323	93.9677	0.433
5	8.3902	82.7341	0.077
6	9.989	90.8879	0.138
7	12.781	88.0023	0.066
8	13.985	86.8745	0.111
9	15.997	83.9978	0.3
10	18.453	82.2348	0.21
11	20.0842	79.8765	0.013

**Table 9.** Analysis of variance for impact strength

Source	DF	SS	MS	% of Contribution
Regression	2	0.00741	0.00371	18.3
Residual Error	8	0.13239	0.01655	81.7
Total	10	0.1398	0.02026	

### 4.3 Modulus of rupture (MOR) analysis

The experimental MOR of the Al-Mg-Si-PKSA composites are presented in Table 10 as also done in the previously discussed mechanical properties. The result also showed variation in MOR of the composite as the composition changes. The mathematical modeling of the experimental MOR is displayed in Equation 8 obtained with the help of regression analysis. The experimental and the modeled impact strength are presented in Figure 5 and this modeling also revealed that the experimental design does not fit wonderfully.

$$\text{MOR} = 149 - 0.775 \text{ PKSA} - 0.894 \text{ Al} - \text{Mg} - \text{Si} \tag{8}$$

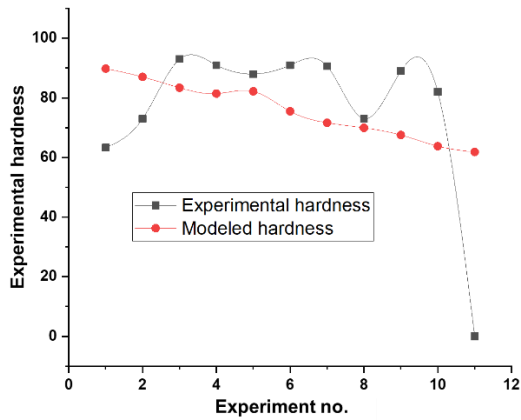


Fig 1. Experimental and Modeled Hardness

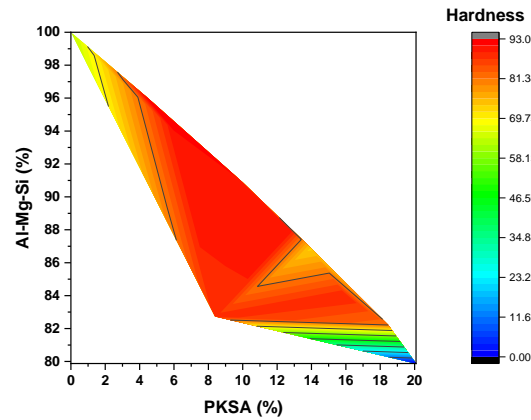


Fig 2. Interaction Plot for Hardness

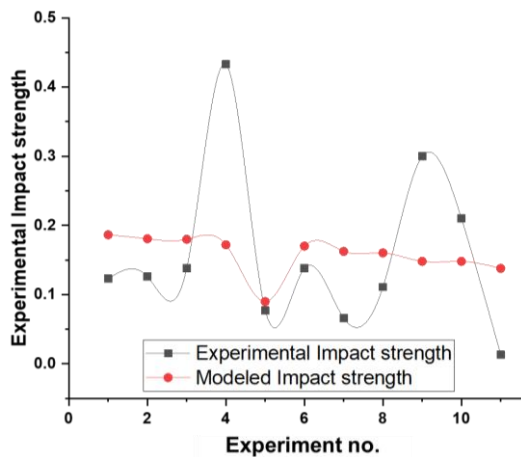


Fig 3. Experimental and Modeled Impact Strength

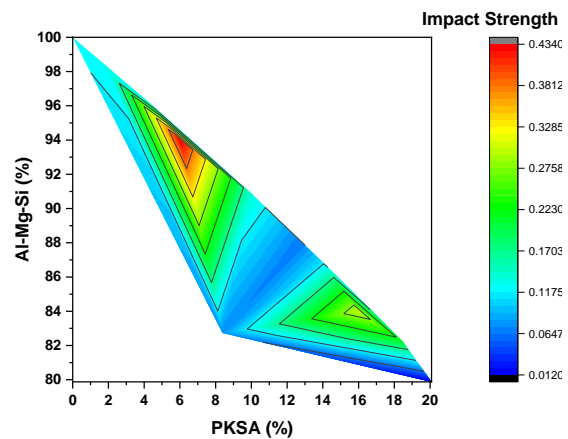


Fig 4. Interaction Plot for Impact Strength

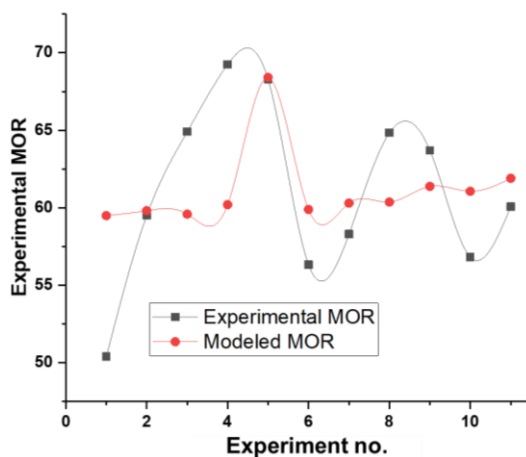


Fig 5. Experimental and Modeled MOR

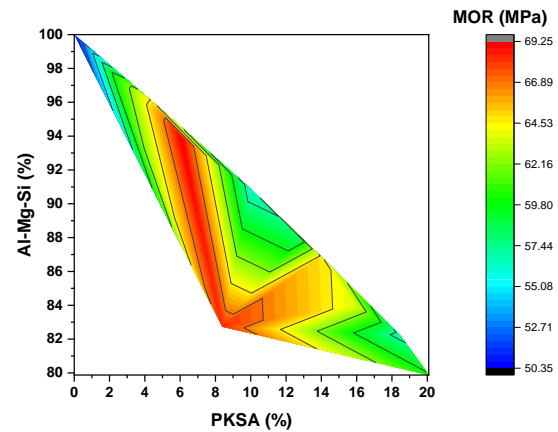


Fig 6. Interaction Plot for MOR



**Table 10.** Experimental MOR

Experiment no.	PKSA	Al-Mg-Si	MOR
1	0	100	50.4
2	2.034	97.874	59.51
3	4.451	96.023	64.91
4	6.0323	93.9677	69.25
5	8.3902	82.7341	68.28
6	9.989	90.8879	56.32
7	12.781	88.0023	58.3
8	13.985	86.8745	64.84
9	15.997	83.9978	63.71
10	18.453	82.2348	56.81
11	20.0842	79.8765	60.07

**Table 11.** Analysis of Variance for MOR

Source	DF	SS	MS	% of Contribution
Regression	2	64.15	32.07	50.02
Residual Error	8	256.31	32.04	49.98
Total	10	320.45	64.11	

The modeling of MOR presented in Figure 5 showed a better fitness of the experiment as compared hardness and impact strength of the composite. However, it is important to note that the residual errors contributed significantly on MOR of the composite. The ANOVA analysis in Table 11 gave a quantitative contribution of the residual error to be 49.98%. As it is recommended in other mechanical properties analysis, further study should be conducted on essential factors responsible on the mechanical properties of Al-Mg-Si composite.

The interaction plot of the compositions showing their corresponding MOR is shown in Figure 6. The results showed an L curve pattern of the composition that gave better with the red color. The presented interaction plot also highlights different compositions of Al-Mg-Si and PKSA with different resultant MOR.

## 5. Conclusion

Mechanical analysis and modeling of Al-Mg-Si-PKSA composite have been successfully done in this study. It was found that the mechanical properties of the composite are inconsistent with variation in the composition. The mathematical and graphical modeling of the mechanical properties of the composite have been presented. The modeling revealed that the experimental mechanical properties are influenced by some external factors that were not considered in this study. Analysis of variance further substantiate the modeling with quantitative analysis. The interaction study of the analyzed mechanical properties showed a broader view of different combination of the compositions with their resultant mechanical properties. It also showed some specific compositions that could result to better mechanical properties. It is strongly recommended that further analysis should be conducted on other essential factors that may be responsible on the mechanical properties of the composite.

## Acknowledgement

The authors will like to acknowledge the support provided by the Departments of Mechanical Engineering and Metallurgical and Materials Engineering, Ahmadu Bello University, Zaria, Nigeria. The data can be made available on a reasonable request.

## Appendix: Nomenclature

Symbol	Description
FSP	Friction stir processing
UFG	Ultrafine-grained
MMC	Metal Matrix Composite

HMMC	Hybrid Metal Matrix Composite
PMMCs	Particulate Metal Matrix Composites
GRA	Grey Relational Analysis
PKSA	Palm Kernel Shell Ash
ASTM	American Society for Testing and Materials
ISO	International Organization for Standardization
m	Meters
s	Seconds
mm	Millimetre
°C	Degree Celsius
ANOVA	Analysis of Variance
MPa	Mega-Pascal
MOR	Modulus of Rupture
J	Joules
$x_i(k)$	Preprocessed data/similarity arrangements
$X_o(k)$	Reference arrangements
$y_i(k)$	Response estimation
$\Delta_{oi}(k)$	Difference in absolute value between $x_o(k)$ and $x_i(k)$
$\zeta$	Distinguishing coefficient of Deng's GRA model
$\Delta_{min}, \Delta_{max}$	The base of every reaction variable
GRC	Grey Relationship Coefficient
GRG	Grey Relational Grade
$P_{ij}$	Partial positive probability index
$\square_j$	Normalized factor
$j^{th}$	utility index of the performance characteristic indicator
$x_{ij}$	$j^{th}$ beneficial utility index of the sample's characteristic performance measurement
$n$	Number of samples in the study
$m$	Number of utility indices for each sample involved
$x_j$	Sample characteristics performance indicator's arithmetic mean utility index
DF	Degree of Freedom
SS	Sum of Squares
MS	Mean Squares

## References

- Abifarin, J. K., Olubiyi, D. O., Dauda, E. T., & Oyediji, E. O. (2021). Taguchi Grey Relational Optimization of the Multi-mechanical Characteristics of Kaolin Reinforced Hydroxyapatite: Effect of Fabrication Parameters. *International Journal of Grey Systems*, 1(2), 20–32. <https://doi.org/10.52812/ijgs.30>
- Chakravarthy, C. H. N., Kumar, S. S., Muthalagu, R., & Ramasamy, M. (2020). Experimental investigation and optimization on surface parameters of ZrO<sub>2</sub> nano particles reinforced Al-7050 metal matrix composites for aeronautical applications. *Materials Today: Proceedings*, 37(Part 2), 2406–2414. <https://doi.org/10.1016/j.matpr.2020.08.265>
- Chaudhary, S., & Tak, R. K. (2022). Natural corrosion inhibition and adsorption characteristics of tribulus terrestris plant extract on aluminium in hydrochloric acid environment. *Biointerface Research in Applied Chemistry*, 12(2), 2603–2617. <https://doi.org/10.33263/BRIAC122.26032617>
- Chou, T., Kelly, A., & Okura, A. (1985). Fibre-reinforced metal-matrix composites. *Composites*, 16(3), 187–206. [https://doi.org/10.1016/0010-4361\(85\)90603-2](https://doi.org/10.1016/0010-4361(85)90603-2)
- Edalati, K., Imamura, K., Kiss, T., & Horita, Z. (2012). Equal-channel angular pressing and high-pressure torsion of pure copper: Evolution of electrical conductivity and hardness with strain. *Materials Transactions*, 53(1), 123–127. <https://doi.org/10.2320/matertrans.MD201109>
- Engler, O. (2022). Effect of precipitation state on plastic anisotropy in sheets of the age-hardenable aluminium alloys AA 6016 and AA 7021. *Materials Science and Engineering A*, 830, 142324. <https://doi.org/10.1016/j.msea.2021.142324>
- Girish, B. M., Siddesh, H. S., & Satish, B. M. (2019). Taguchi grey relational analysis for parametric optimization of severe plastic deformation process. *SN Applied Sciences*, 1(8), 1–11. <https://doi.org/10.1007/s42452-019-0982-6>
- Kazemi-Navaee, A., Jamaati, R., & Aval, H. J. (2021). Asymmetric cold rolling of AA7075 alloy: The evolution of microstructure, crystallographic texture, and mechanical properties. *Materials Science and Engineering A*, 824, 141801. <https://doi.org/10.1016/j.msea.2021.141801>
- Kordijazi, A., Zhao, T., Zhang, J., Alrfou, K., & Rohatgi, P. (2021). A Review of Application of Machine Learning in Design, Synthesis, and Characterization of Metal Matrix Composites: Current Status and Emerging Applications. *Jom*, 73(7), 2060–2074. <https://doi.org/10.1007/s11837-021-04701-2>
- Kulekci, M. K. (2008). Magnesium and its alloys applications in automotive industry. *International Journal of Advanced Manufacturing Technology*, 39(9–10), 851–865. <https://doi.org/10.1007/s00170-007-1279-2>
- Li, Q., Xue, S., Wang, J., Shao, S., Kwong, A. H., Giwa, A., Fan, Z., Liu, Y., Qi, Z., Ding, J., Wang, H., Greer, J. R., Wang, H., & Zhang, X. (2018). High-Strength Nanotwinned Al Alloys with 9R Phase. *Advanced Materials*, 30(11), 1704629. <https://doi.org/10.1002/adma.201704629>
- Miracle, D. B. (2005). Metal matrix composites - From science to technological significance. *Composites Science*

- and Technology, 65(15-16 SPEC. ISS.), 2526–2540. <https://doi.org/10.1016/j.compscitech.2005.05.027>
- Oyedede, A. N., Umar, A. U., Kuburi, L. S., & Apeh, I. O. (2020). Trend of Harvesting of Oil Palm Fruit; The Mechanisms, and Challenges. *International Journal of Scientific Research and Engineering Development*, 3(3), 1053–1063. <http://www.ijrsred.com/volume3/issue3/IJSRED-V3I3P138.pdf>
- Oyedede, A., Umar, U. A., & Shettima, K. L. (2021a). Investigation of the Allometry of Oil Palm Trees in Nigeria for Mechanization of the Farming Process. *Atbuftejoste.Com*, 9(2), 123–130. <http://www.atbuftejoste.com/index.php/joste/article/view/1205>
- Oyedede, E., Dauda, M., Yaro, S., & Abdulwahab, M. (2021b). Palm Kernel Shell Ash Particle Reinforcement on Al-Mg-Si and its Effect on the Mechanical and Thermal Behaviour. *Journal of Experimental Research*, 9(2), 57–66.
- Oyedede, E. O., Dauda, M., Yaro, S. A., & Abdulwahab, M. (2022). The effect of palm kernel shell ash reinforcement on microstructure and mechanical properties of Al-Mg-Si metal-matrix composites. *Proceedings of the Institution of Mechanical Engineers, Part C: Journal of Mechanical Engineering Science*, 236(3), 1666–1673. <https://doi.org/10.1177/09544062211014535>
- Oyedede, Elijah O, Dauda, M., Yaro, S. A., & Abdulwahab, M. (2021c). Influence of Particle Size and Particle Range Distribution on the Microstructure of Al–Mg–Si/PKSA Composite for Amateur Solid Rocket Chamber. *FUOYE Journal of Engineering and Technology*, 6(1), 88-91. <https://doi.org/10.46792/fuoyejet.v6i1.580>
- Pandya, V. J., & Rathod, P. P. (2020). Optimization of mechanical properties of green composites by gray relational analysis. *Materials Today: Proceedings*, 27, 19–22. <https://doi.org/10.1016/j.matpr.2019.08.166>
- Rakhmonov, J., Liu, K., Rometsch, P., Parson, N., & Grant Chen, X. (2021). Effects of Al (MnFe) Si dispersoids with different sizes and number densities on microstructure and ambient/elevated-temperature mechanical properties of extruded Al. *Journal of Alloys and Compounds*, 861, 157937. <https://doi.org/10.1016/j.jallcom.2020.157937>
- Ramu, I., Srinivas, P., & Vekatesh, K. (2018). Taguchi based grey relational analysis for optimization of machining parameters of CNC turning steel 316. *IOP Conference Series: Materials Science and Engineering*, 377(1), 012078. <https://doi.org/10.1088/1757-899X/377/1/012078>
- Reddy, S., & Chalamalasetti, S. R. (2021). Optimization of drilling parameters during machining of Al-Mg-Si alloys by Taguchi method coupled with grey relational analysis and validated by FEA based deform - 3D. *Strojnický Casopis*, 71(2), 221–238. <https://doi.org/10.2478/scjme-2021-0032>
- Sanchez, J. M., Pascual, A., Vicario, I., Albizuri, J., Guraya, T., & Galarraga, H. (2021). Microstructure and phase formation of novel Al80Mg5Sn5Zn5X5 lightweight complex concentrated aluminum alloys. *Metals*, 11(12), 1944. <https://doi.org/10.3390/met11121944>
- Sharma, S., Singh, J., Gupta, M. K., Mia, M., Dwivedi, S. P., Saxena, A., Chattopadhyaya, S., Singh, R., Pimenov, D. Y., & Korkmaz, M. E. (2021). Investigation on mechanical, tribological and microstructural properties of Al-Mg-Si-T6/SiC/muscovite-hybrid metal-matrix composites for high strength applications. *Journal of Materials Research and Technology*, 12, 1564–1581. <https://doi.org/10.1016/j.jmrt.2021.03.095>
- Soorya Prakash, K., Gopal, P. M., & Karthik, S. (2020). Multi-objective optimization using Taguchi based grey relational analysis in turning of Rock dust reinforced Aluminum MMC. *Measurement: Journal of the International Measurement Confederation*, 157, 107664. <https://doi.org/10.1016/j.measurement.2020.107664>
- Sumesh, K. R., & Kanthavel, K. (2020). Optimizing various parameters influencing mechanical properties of banana/coir natural fiber composites using grey relational analysis and artificial neural network models. *Journal of Industrial Textiles*. <https://doi.org/10.1177/1528083720930304>
- Yin, M. S. (2013). Fifteen years of grey system theory research: A historical review and bibliometric analysis. *Expert Systems with Applications*, 40(7), 2767–2775. <https://doi.org/10.1016/j.eswa.2012.11.002>